Chaos due to homoclinic and heteroclinic orbits in two coupled oscillators with nonisochronism

Maxim Poliashenko and Susan R. McKay
Department of Physics and Astronomy, University of Maine, Orono, Maine 04469
(Received 20 April 1992)

We show that chaotic dynamics occur in a pair of weakly nonlinear coupled active oscillators when nonisochronism, the dependence of oscillation frequencies on amplitudes, is included. The strange attractor in this system develops from a nearby homoclinic orbit, the same mechanism that leads to chaos in coupled active-passive modes. After analytically determining the most likely parameter region for such a homoclinic orbit, we found the neighboring region of chaos predicted by Shilnikov's theorem. These coupled oscillators also exhibit multistability and unexpected three-frequency oscillations.

PACS number(s): 05.45.+b, 84.20.+m, 84.30.Ng, 03.20.+i

Coupled oscillators provide fundamental models of the dynamics of many biological, chemical, and physical systems. The addition of weak nonlinearity in these systems produces a variety of dramatically different complex dynamical features, particularly in cases in which nonisochronism, the dependence of frequencies upon amplitudes of the oscillators, is included.

Recently, we have shown that a system of two nonisochronous active-passive oscillators exhibits chaotic dynamics [1], but no chaotic region had previously been detected for coupled active modes. Here we first establish that chaos in the active-passive system arises from the Shilnikov mechanism [2–4]. By investigating the possibility that this mechanism could be present in the case of coupled active modes, we have been able to locate the much more elusive chaotic region in this case.

Over 20 years ago, Shilnikov proved that a saddle-focus homoclinic orbit under certain conditions has in its neighborhood a countable set of periodic trajectories which can lead to the formation of a chaotic attractor. For chaos to occur within a three-dimensional phase space, Shilnikov's work requires that the homoclinic's equilibrium point, with eigenvalues $-\delta$ and $\gamma\pm i\omega$, must have $\delta>\gamma>0$. Although this mechanism for chaos has been known theoretically for a long time, it has only recently been identified in physical systems, such as electrical oscillatory circuits [5] and single-mode lasers [6]. It is often recognized by the orbits with long periods which exist in parameter ranges close to the homoclinic orbit.

In the present study, we show how Shilnikov chaos arises in a fundamental system consisting of two weakly nonlinear coupled oscillators with dynamics described by the following differential equations:

$$\begin{aligned}\ddot{x}_1-\epsilon_1 F_1(x_1,x_2)\dot{x}_1+\omega_1^2 G_1(x_1,x_2)x_1=Kx_2\ ,\\ \ddot{x}_2-\epsilon_2 F_2(x_1,x_2)\dot{x}_2+\omega_2^2 G_2(x_1,x_2)x_2=Kx_1\ ,\end{aligned}\tag{1}$$

where F_i and G_i are even functions with one maximum. In the limit of weak nonlinearity, these functions can be approximated by second-order polynomials:

$$\begin{aligned}F_i(x_1,x_2)&=1-\nu_i x_1^2-\rho_i x_2^2\ ,\\ G_i(x_1,x_2)&=1-\delta_i x_1^2-\sigma_i x_2^2\ ,\quad i=1,2\ .\end{aligned}\tag{2}$$

If the two oscillators are weakly coupled and weakly nonlinear, solutions of Eq. (1) can be written with slowly varying amplitudes and phases, as introduced by Van der Pol [7],

$$\begin{aligned}x_1(t)&=a(t)\cos[\omega t+\phi_1(t)]\ ,\\ x_2(t)&=b(t)\cos[\omega t+\phi_2(t)]\ ,\end{aligned}\tag{3}$$

where $a(t)$ and $b(t)$ are the amplitudes and $\phi_1(t)$ and $\phi_2(t)$ are the phases of the two oscillators, which vary slowly in time compared with $\cos(\omega t)$. First-order averaging methods [8,9] then yield the following equations for the amplitudes and the phase difference $\psi\equiv\phi_2-\phi_1$:

$$\begin{aligned}\frac{da}{d\tau}&=(\alpha_a-\gamma_a a^2-\mu_a b^2)a+kb\sin\psi\ ,\\ \frac{db}{d\tau}&=(\alpha_b-\gamma_b b^2-\mu_b a^2)b-ka\sin\psi\ ,\\ \frac{d\psi}{d\tau}&=-\Delta+\beta a^2-\kappa b^2+k\left[\frac{b}{a}-\frac{a}{b}\right]\cos\psi\ .\end{aligned}\tag{4}$$

Here, τ is the "slow" time, Δ is proportional to the detuning of the two partial frequencies, and α_a and α_b characterize the linear, and γ_a,γ_b the nonlinear, dissipation of the oscillators. In particular, an oscillator with negative (positive) α exhibits an amplitude that is damped (increasing) in the linear approximation, yielding a passive (active) mode. The coefficients β and κ represent nonisochronous features of the oscillators.

System (4) includes two different coupling mechanisms between the oscillator amplitudes a and b: resonant and nonresonant. The resonant coupling occurs through the phase difference ψ and its strength is controlled by the coupling constant k. Nonresonant coupling of the two modes links the two amplitudes directly through terms with $\mu_{a,b}$ and does not depend upon the phase difference.

 ©1992 The American Physical Society

Similar equations have been derived previously [5] and can be obtained by other first-order asymptotic methods [7,8,10].

The equilibrium states $a=A$, $b=B$, $\psi=\Psi$ of Eq. (4) are situated along the two branches of the resonant curve

$$\Delta=\beta A^2-\kappa B^2\pm\left[\frac{B^2}{A^2}-1\right]\times\left[\frac{k^2A^2}{B^2}-(\alpha_b-\gamma_b B^2-\mu_b A^2)^2\right]^{1/2}, \tag{5}$$

where

$$B^2=\frac{1}{2\gamma_b}(\alpha_b-A^2(\mu_a+\mu_b)\pm\{[\alpha_b-A^2(\mu_a+\mu_b)]^2+4\gamma_b A^2(\alpha_a-\gamma_a A^2)\}^{1/2}).$$

Equation (4) also has a trivial equilibrium point, $A=B=0$ and Ψ undefined. The stability of each fixed point can be determined analytically by calculating the eigenvalues of system (4), linearized about the fixed point. Hopf and saddle-node bifurcations were located analytically using Routh-Hurwitz conditions.

Figure 1 shows the resonance curve corresponding to an active-passive case of system (4). Within the parameter range $-22.562<\Delta<-16.246$, Eq. (4) has only one nontrivial equilibrium point, the saddle-focus point at the center of the lower spiral in Fig. 2(a). From the saddle-node bifurcation, a pair of fixed points emerges with the same complex-conjugate eigenvalues ($-1.237\pm19.531i$) and with real eigenvalues close to zero but of opposite signs. One of them represents a stable steady state, and the other is a saddle focus, the point whose existence is anticipated by the behavior of the trajectory at the upper spiral of Fig. 2(a).

The regular orbit of Fig. 2(a) resembles a classic heteroclinic orbit. The center of the lower spiral is a saddle-focus equilibrium point of Eq. (4) with one eigenvalue real and negative and a complex-conjugate pair of

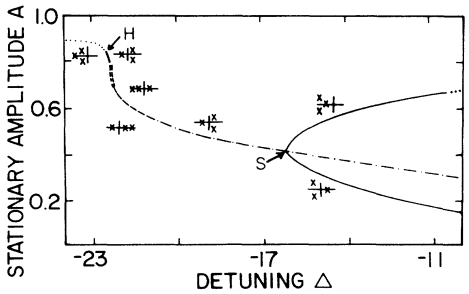

FIG. 1. Equilibrium states for an active-passive case of system (4) with parameter values $\alpha_a=3.0$, $\alpha_b=-1.0$, $\gamma_a=\gamma_b=\mu_a=\mu_b=\beta=0.3$, $\kappa=10.0$, $k=6.5$. Each line style indicates a different type of equilibrium. For each, the eigenvalue positions in the complex plane are indicated by ×'s. Saddle-node and Hopf bifurcation thresholds are marked by S and H respectively.

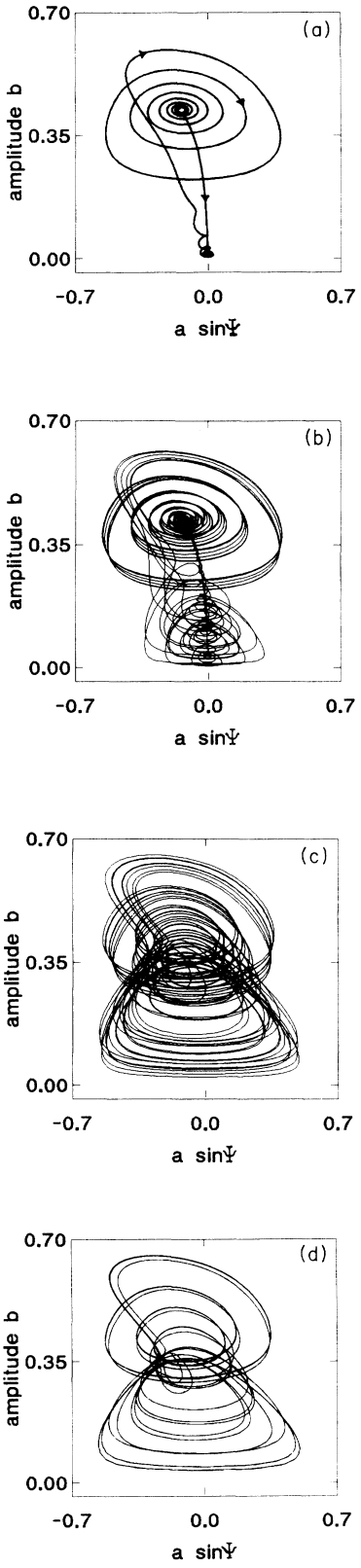

FIG. 2. Regular and chaotic attractors for the active-passive case of system (4). For (a)–(e), parameters are those of Fig. 1; the frequency detuning Δ is equal to (a) -16.30, (b) -16.80, (c) -21.50, (d) -22.40, and (e) -20.60. For (f), $\alpha_a=3.8$, $\alpha_b=-1.2$, $\gamma_a=1.5$, $\gamma_b=0.8$, $\mu_a=2.0$, $\mu_b=\beta=0.0$, $\kappa=100.0$, $k=22.0$, and $\Delta=-62.0$.

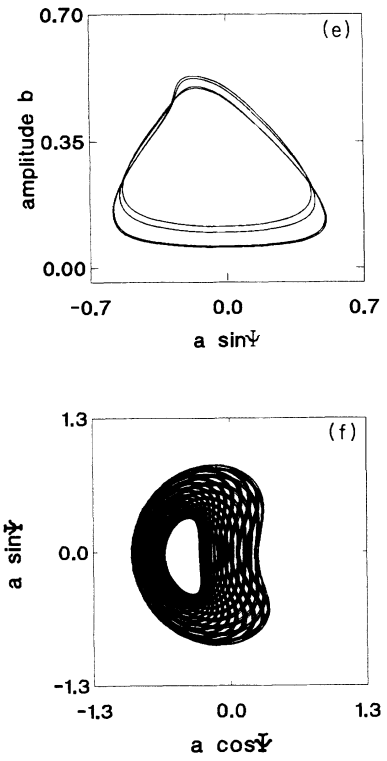

FIG. 2. (*Continued*).

eigenvalues with a positive real part, $\lambda_1 = -11.88$ and $\lambda_{2,3} = 4.93 \pm 5.73i$ for $\Delta_c = -16.225$. Thus, the phase-space trajectory approaches this point along the eigenvector corresponding to the real eigenvalue, and then exits by spiraling until it reaches the basin of attraction of the upper saddle-focus point with eigenvalues 0.04 and $-1.21 \pm 9.43i$ for Δ_c. Then, the trajectory spirals toward this point and stays for a long time in its vicinity before returning to the lower equilibrium point. As Δ approaches Δ_c, the time spent near the vortex of the upper spiral approaches infinity. The shape of this orbit suggests that a heteroclinic orbit also forms for other parameter values. Although the Shilnikov eigenvalue conditions have not yet been formulated for a heteroclinic connection, in our case eigenvalues of at least one saddle-focus equilibrium point do satisfy the Shilnikov conditions.

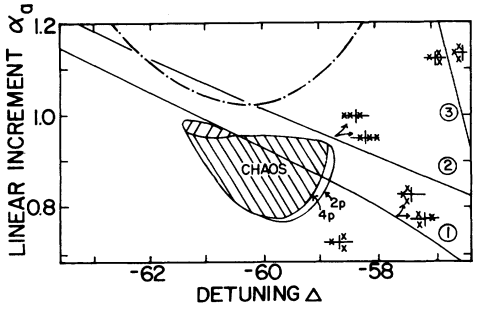

FIG. 3. Bifurcation diagram of system (4) as α_a is varied, with $\alpha_b = \gamma_a = \gamma_b = k = 1$, $\mu_a = \mu_b = \beta = 0$, and $\kappa = 50$. The dot-dashed curve depicts conditions (6). Lines 1 and 2 denote thresholds of saddle-node bifurcations. The Hopf bifurcation threshold is denoted by line 3. The two hatched regions indicate locations of chaos and orbits of homoclinic origin (above chaos). 2p and 4p indicate period-doubling thresholds.

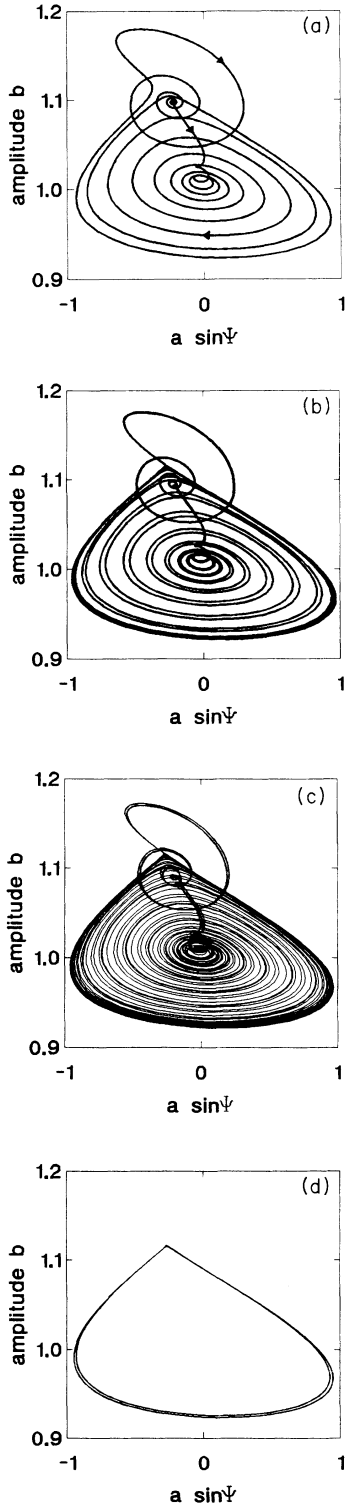

FIG. 4. Regular and chaotic attractors for the active-active case of system (4) with parameters as in Fig. 3 with $\alpha_a = 1$ and with Δ equal to (a) -61.3000, (b) -61.4480, (c) -61.4490, and (d) -61.4492.

Formation of such an orbit can imply the presence of a strange attractor in the neighboring parameter space. Indeed, increasing the magnitude of the detuning leads to the formation of this attractor [Figs. 2(b) and 2(c)]. Chaos is well developed in this region, with a maximal Lyapunov exponent of about 0.05. These chaotic regions are interrupted by numerous windows of order with periodic orbits, such as Fig. 2(d), which subsequently undergo cascades of period doubling, returning to chaos.

Another attractor is the limit cycle [Fig. 2(e)] that appears via the Hopf bifurcation at $\Delta=-22.562$ and coexist with the regular and chaotic attractors discussed above almost throughout the entire parameter range. At certain points, this limit cycle merges into the chaotic attractor and then is subsequently recovered through an inverse sequence of period doublings. Such bistability is typical for these coupled oscillator systems in both the active-passive and active-active modes.

Guided by these results from the active-passive case, we decided to look for homoclinic orbits in the case of two active oscillators, since the development of chaos might be due to the same mechanism in the two cases. In a previous study [11], we had used an asymptotic method to determine the boundaries of competition between a stable fixed point and a stable periodic orbit for this system. There the dynamics of Eq. (4) for large κ and $\beta=\mu_a=\mu_b=0$ were shown to be well approximated by a nonlinear pendulum equation. Within this approximation, the condition for two separatrices to form a heteroclinic loop in the phase plane of that equation is

$$\frac{\gamma}{(\zeta^2-\gamma^2)^{1/4}}=\tfrac{3}{8}\pi\nu\ , \tag{6}$$

with

$$\nu=3\gamma_b B^2-\alpha_b\ ,\quad \zeta=-2\kappa ABk\ ,\quad \gamma=2\kappa B^2(\gamma_b B^2-\alpha_b)\ . \tag{7}$$

For system (4), with $\Psi\in[0,2\pi]$, Eq. (6) means that a homoclinic orbit has formed. Figure 3 shows a bifurcation diagram for Eq. (4) for $\alpha_a,\alpha_b>0$ in the parameter plane (Δ,α_a). Lines labeled 1 and 2 indicate saddle-node bifurcations, and line 3 shows the Hopf bifurcation threshold. The dash-dot curve traces parameter values where condition (6) holds. For values of $\alpha_a\approx 1.05$, the curve flattens, forming a broad minimum. In this vicinity, a homoclinic orbit could form over a relatively wide range of detuning Δ. One would expect orbits with long periods close to the homoclinic orbit, due to the continuity of solutions as parameters are changed. By numerically searching this parameter region, the expected long-period orbits were found [Fig. 4(a)]. They do look structurally identical to those found for the active-passive case, approaching a homoclinic orbit as Δ goes to -61.2525. In a parameter space region near these orbits, chaotic dynamics occur (Fig. 3), in the vicinity of the extremum of Eq. (6), as hypothesized.

The dynamics of active-active and active-passive systems show further similarities. In both cases, a simple limit cycle and a limit cycle of homoclinic origin coexist within a certain parameter range. As Δ approaches the threshold of the saddle-node bifurcation, the "soon-to-emerge" fixed point in the upper spiral attracts the phase trajectory with increasing strength, which causes bending and folding of the limit cycle, eventually initiating a sequence of period doubling bifurcations [Fig. 4(d)]. This cascade finishes with the formation of a band-type chaotic attractor. With further increases in Δ, intermittency occurs between this attractor and the limit cycle of homoclinic origin. The length of chaotic bursts grows, eventually leading to the formation of the strange attractor [Fig. 4(c)]. This attractor goes through an inverse sequence of period doublings [Fig. 4(b)] and approaches a homoclinic orbit [Fig. 4(a)]. As in the case of active-passive oscillators, this orbit also coexists with a simple limit cycle which appears as a result of the Hopf bifurcation.

Bistability and multistability are typical within the parameter regions where chaos occurs. For instance, for the active-passive case, the chaotic attractor coexists with a stable equilibrium and with a limit cycle, so one-frequency, two-frequency, and chaotic oscillations are all possible for the same parameter values.

It is noteworthy that the active-passive system also displays *three-frequency* oscillations. Figure 2(f) displays quasiperiodic oscillations, indicating three-frequency dynamics in the original system, Eq. (1). This phenomenon is unexpected for a weakly nonlinear system with two degrees of freedom, but has been previously observed in electrical oscillatory circuits [12].

We thank M. Friedman for providing unpublished results of his numerical investigations of homoclinic and heteroclinic orbits in this system and B. Deng for helpful discussions.

[1] M. Poliashenko, S. R. McKay, and C. W. Smith, Phys. Rev. A **44**, 3452 (1991).
[2] I. M. Ovsyannikov and L. P. Shilnikov, Math. USSR Sbornik **58**, 557 (1987).
[3] L. P. Shilnikov, Math. USSR Sbornik **10**, 91 (1970); Sov. Math. Dokl. **8**, 102 (1967).
[4] B. Deng, SIAM J. Math. Anal. **21**, 693 (1990).
[5] A. B. Belogortsev, D. M. Vavriv, and O. A. Tretyakov, Radiophys. Quantum Electron. **33**, 187 (1990).
[6] C. O. Weiss, N. B. Abraham, and U. Hübner, Phys. Rev. Lett. **61**, 1587 (1988).
[7] B. Van der Pol, Philos. Mag. **43**, 700 (1922).
[8] N. M. Krylov and N. N. Bogoliubov, *Introduction to Nonlinear Mechanics* (Princeton University, Princeton, 1947); N. N. Bogoliubov and Yu. A. Mitropolsky, *Asymptotic Methods in the Theory of Nonlinear Oscillations* (Gordon and Breach, New York, 1961).
[9] J. Guckenheimer and P. Holmes, *Nonlinear Oscillations, Dynamical Systems and Bifurcations of Vector Fields* (Springer-Verlag, New York, 1984), Chap. 4.
[10] R. H. Rand and P. J. Holmes, Int. J. Non-Linear Mech. **15** 387 (1980).
[11] M. Poliashenko, S. R. McKay, and C. W. Smith, Phys. Rev. A **43**, 5638 (1991).
[12] I. Yu. Cherneshov and D. M. Vavriv (unpublished).

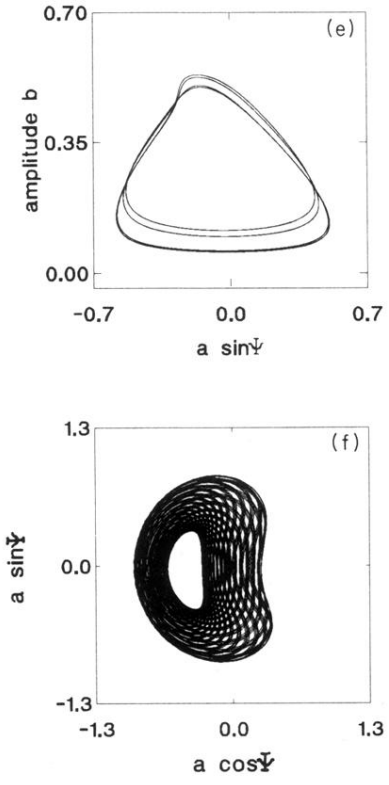

FIG. 2. (*Continued*).

eigenvalues with a positive real part, $\lambda_1 = -11.88$ and $\lambda_{2,3} = 4.93 \pm 5.73i$ for $\Delta_c = -16.225$. Thus, the phase-space trajectory approaches this point along the eigenvector corresponding to the real eigenvalue, and then exits by spiraling until it reaches the basin of attraction of the upper saddle-focus point with eigenvalues 0.04 and $-1.21 \pm 9.43i$ for Δ_c. Then, the trajectory spirals toward this point and stays for a long time in its vicinity before returning to the lower equilibrium point. As Δ approaches Δ_c, the time spent near the vortex of the upper spiral approaches infinity. The shape of this orbit suggests that a heteroclinic orbit also forms for other parameter values. Although the Shilnikov eigenvalue condi-

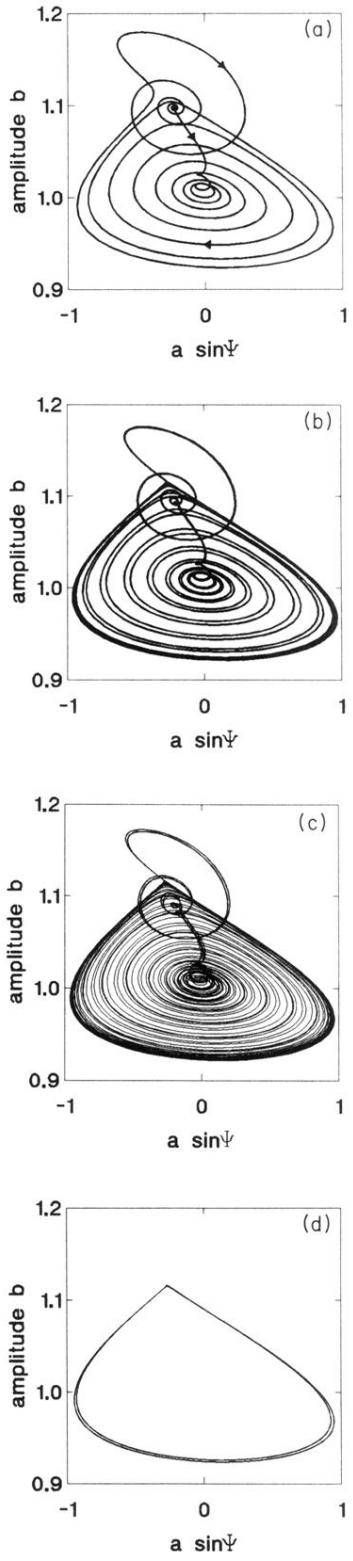

FIG. 4. Regular and chaotic attractors for the active-active case of system (4) with parameters as in Fig. 3 with $\alpha_a = 1$ and with Δ equal to (a) -61.3000, (b) -61.4480, (c) -61.4490, and (d) -61.4492.